Thermomechanical Characterization of a TiPdNi High Temperature SMA under Tension

Parikshith K. Kumar[a] , Dimitris C. Lagoudas[b]

[a] Graduate Student, Aerospace Engineering, Texas A & M University, College Station, Texas 77843
[b] John and Bea Slattery Chair, Professor, Aerospace Engineering, Texas A & M University, College Station, Texas 77843

ABSTRACT

The focus of this paper is the study of tensile work characteristics and the transformation behavior of a High Temperature Shape Memory Alloy (HTSMA) by thermomechanical characterization at temperatures ranging from 200 to 500°C. In order to investigate the above issues, a nominal composition of $Ti_{50}Pd_{40}Ni_{10}$ HTSMA was used. The alloy was fabricated using a vacuum arc melting technique. The melt was cast and hot rolled followed by cutting of tensile specimen using Electrode Discharge Machining (EDM). A high temperature experimental setup was developed on a load frame to test the material at high temperatures under constrained actuation conditions. The stability of the material response under cyclic actuation was also investigated. The observations from the tests are presented in this paper. Microprobe analysis was performed on the as-cast and rolled material to study the composition. The material was also studied by X-ray diffraction (XRD) and optical microscopy before and after testing. Certain key observations about the material response are discussed specifically, in terms of transformation behavior, recoverable strains under various applied total strains, and cyclic thermomechanical behavior.

Keywords: Thermomechanical characterization, High Temperature, HTSMA, TiPdNi.

1. INTRODUCTION

Shape Memory Alloys (SMAs) have been a widely studied active material for actuators and sensors for the past several decades due to the unique properties they exhibit, namely the Shape Memory Effect (SME) and the pseudoelastic effect [1, 2]. The growing demand for actuation mechanisms in higher temperature environments driven by the aerospace [3] and the oil industries [4] has led to a new class of SMAs known as High Temperature Shape Memory Alloys (HTSMAs). The addition of ternary elements such as Palladium, Platinum, Hafnium, Gold or Zirconium to binary NiTi [5-8] can shift the transformation temperatures above 100°C to create a new range of HTSMAs with M_s transformation temperatures as high as 1000 °C [9].

Since the early study of phase transformation behavior in Au-Ti, Pd-Ti and Pt-Ti [10], several binary alloy compositions have been investigated for use as HTSMA actuators [5, 7, 11]. These early studies focused on studying the shape memory behavior of the material, however, poor shape memory behavior was observed in most binary HTSMAs such as NiAl and TiPd with increased test temperatures [11, 12]. Techniques such as alloying, thermomechanical treatment, and processing have since been adopted to improve the behavior of these materials [13-15]. Different compositions of TiPdNi alloy have shown improved shape memory behavior after precipitation hardening and thermomechanical treatments [13, 15]. Until recently, most efforts studied the recoverable behavior of the material under zeros stress conditions. Recent efforts on HTSMAs have focused on studying and improving the work characteristics of the TiPdNi and TiPtNi alloys by increasing the critical stress for slip [16-19]. Improved techniques have also been developed to process the material in different forms [20].

The primary focus of this work is to study the tensile thermomechanical behavior of $Ti_{50}Pd_{40}Ni_{10}$ HTSMA for potential use in actuator applications. The choice for the material was governed by its need to operate between 300°C to 500°C. For applications requiring high temperature actuation such as chevrons [21] in the core region of a jet engine or for down-hole applications in the oil industry, it is necessary to have knowledge of the operational capabilities of the HTSMA actuator. Earlier work has shown this alloy composition to produce recoverable strains up to approximately 3.0

% under zero load [13]. Recent efforts have focused on studying the work characteristics of these materials in detail. Previous study on the compressive behavior of $Ti_{50}Pd_{40}Ni_{10}$ [16] had shown a strong dependence of actuation strain on applied strain and actuation stress level. Following the work on studying the work characteristics in compression, the focus of this effort is to study in detail the effect of the transformation behavior in TiPdNi under tensile stress. The effect of applied strain and the cyclic actuation behavior of the HTSMA will be investigated.

The paper is organized as follows: Section 2 describes alloy fabrication and the experimental procedure. The experimental results are presented in Section 3. Section 4 involves a detailed discussion of the results with associated tests to support the hypothesis. The results are then summarized and the conclusions are presented in Section 5.

2. FABRICATION AND EXPERIMENTAL PROCEDURE

2.1 – DSC and Microprobe Analysis

An ingot of a $Ti_{50}Pd_{40}Ni_{10}$ was cast by vacuum arc technique by melting individual metals of purity 99.99% Ti, 99.95% Pd and 99.99% Ni in a water-cooled copper hearth. The ingot was re-melted three times and homogenized at 1000°C for 18ks. The cast bar was then hot rolled at 900 °C with a total thickness reduction of 30% carried out in multiple steps. Samples of the material from both the pre and post rolled material were cut using a low speed diamond saw and analyzed in a Pyris 1 DSC to determine the transformation temperatures. Microprobe analysis was also conducted on the material before and after rolling to study the composition distribution in the microstructure. After rolling, Electrode Discharge Machining (EDM) was used to fabricate tensile dog bone specimens with a gauge length of 1x3x8 mm.

2.2 – Thermomechanical Testing

A high temperature test system was developed for tensile testing at temperatures ranging from room temperature (22 °C) to 600 °C. Figure 1 shows the experimental setup used for testing. The temperature of the specimen was monitored using a high temperature thermocouple that was in contact with the specimen surface.

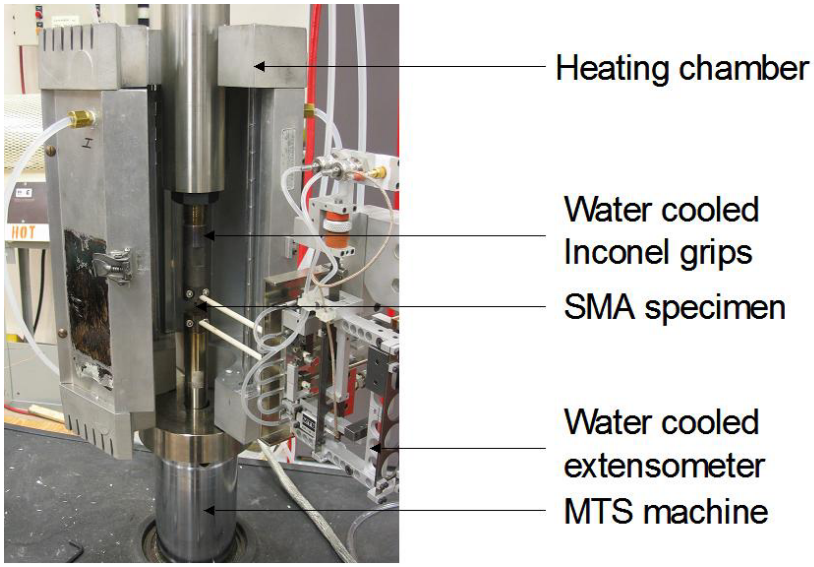

Figure 1. Experimental setup used for testing HTSMA showing water-cooled tension grips, extensometer and water-cooled quartz furnace.

The grips used in the setup were made out of precipitation hardened Inconel (Inconel 718 AMS 5663) to avoid effects of the softening of the grips. The top grip was water-cooled to prevent excessive thermal expansion during the heating

process. The bottom grip rested on a steel plate, which supported the furnace (Model E4 Quad elliptical heating chamber) and dissipated heat from the bottom grip. The strain was measured using a high temperature extensometer (MTS 632.59B-01) with the ceramic leads spring-loaded on the gripping region of the specimen. The furnace and the extensometer were water-cooled to avoid overheating of these components during testing.

For the design of an actuator, understanding the effects of applied strain and the amount of recoverable strain under different stress levels is crucial. In order to study the effect of applied strain on the tensile actuation behavior, the specimen was isothermally loaded to a predefined total applied strain AB in the martensitic state. The equivalent path AB as represented along the stress axis is shown in the loading path represented in the phase diagram (Figure 2). Following this the specimen was unloaded to a stress level C. The specimen was held under constant stress and heated to the point D above the austenitic finish temperature. The specimen was then cooled to the test temperature C (below M_f). The specimen was thermally cycled between temperatures C and D under constant stress. Following the thermal cycling, the specimen was isothermally unloaded to zero stress level in the martensitic state (denoted by A). Next, the stress was held constant at zero and the specimen was heated from martensitic state to austenite temperature E to recover any remnant-detwinned martensite. The specimen was subsequently cooled and the material was thermally cycled under zero stress to observe any TWSME if exhibited. The same loading path was repeated for different applied strain levels AB.

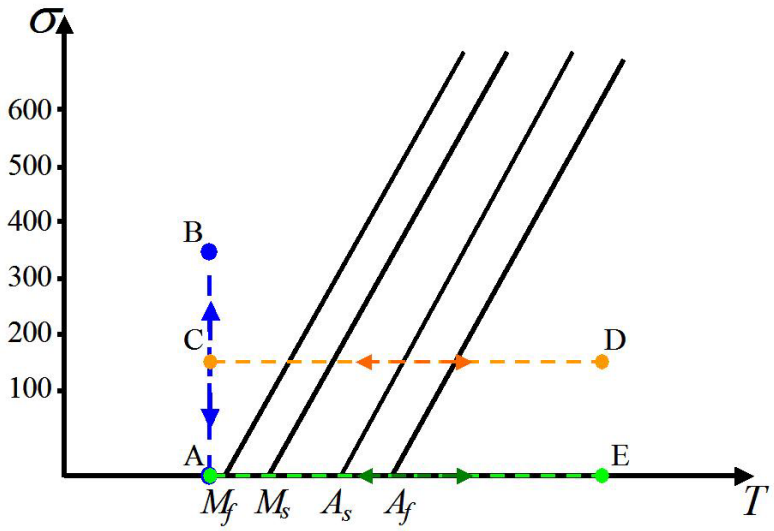

Figure 2. Thermomechanical loading path ABCDCAE represented on a Stress-temperature phase diagram.

3. EXPERIMENTAL RESULTS

3.1 – DSC and Microprobe Analysis

The transformation temperatures for both the as-cast and the rolled material are shown in Figure 3. From the two DSC measurements it is noted that the post rolled sample shows a decrease in the peak temperatures and widening between the start and finish transformation temperatures during both heating and cooling as compared to the as-cast material. The martensitic finish temperatures are difficult to determine from the post-rolled DSC data. Preliminary microprobe analysis on the post-rolled material as compared to the pre-rolled indicated the formation of large Ti rich-Pd, Ti rich-Ni precipitate in the post rolled bar. Also, the content of Ti in the matrix is lowered. Table 1 shows the composition measurements for the pure matrix and the precipitate regions. The lowering of Ti content in the matrix may have occurred due to the diffusion of Ti from the matrix to form precipitates. This variation in Ti content could have resulted in widening of the transformation behavior with a decrease in the transformation temperatures.

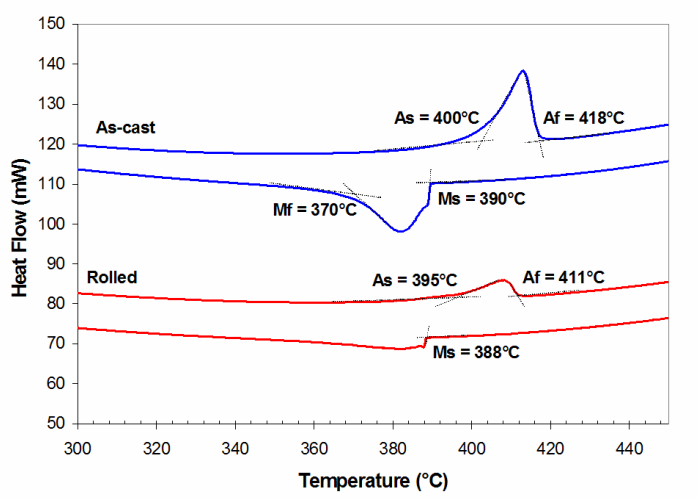

Figure 3. DSC graph showing transformation temperatures for the as-cast and the rolled TiPdNi sample.

Type	Ti (at.%)	Pd (at.%)	Ni (at.%)
Matrix	45.97	43.05	10.92
Matrix	45.64	43.44	10.80
Matrix	45.84	42.88	11.13
Precipitate	61.08	24.21	14.63
Precipitate	63.28	19.01	17.59

Table 1. Composition of matrix and precipitate determined by microprobe analysis on post-rolled specimen.

3.2 – Thermomechanical testing

Figure 4a represents the stress-strain curve based on the loading path described in the earlier section for a 5% applied initial strain. Figure 4b represents the strain-temperature under a constant stress level of 150 MPa after the 5% strain is applied. Figure 4c represents the strain-temperature behavior of the sample after it is unloaded and thermally cycled at zero constant stress. The test begins with the specimen held at a constant temperature of 260ºC in the martensitic state. A 5% strain is applied to the specimen after which the specimen is unloaded to 150 MPa as seen in Figure 4a. The specimen is then held at a constant stress of 150 MPa and thermally cycled through the full transformation. During the first heating cycle above A_f, the tensile specimen increases in length (Figure 4b). On cooling the specimen expands further, resulting in approximately 7% total increase in strain during the first thermal cycle. Subsequent thermal cycling results in the contraction (during heating), and expansion (during cooling) as expected from a conventional SMA under tensile loading. Following the thermal cycling under stress, the material is elastically unloaded to zero stress in the martensitic state. The material is heated under a constant zero stress to recover any residual martensite. On heating above A_f, the specimen now contracts as expected however there is an additional contraction of the specimen upon cooling. The recovered strain in the specimen during the first thermal cycle in the absence of stress was approximately 9%. Subsequent thermal cycling results in expansion (on heating) and contraction (on cooling) with a cyclic recoverable strain of about 4%. The test was repeated with different applied initial strain levels of 1% and 4%. The results were consistent with the behavior observed in the case of the 5% applied strain. The evolution of transformation strain in each cycle (under stress) for different levels of applied strains is shown in Figure 5.

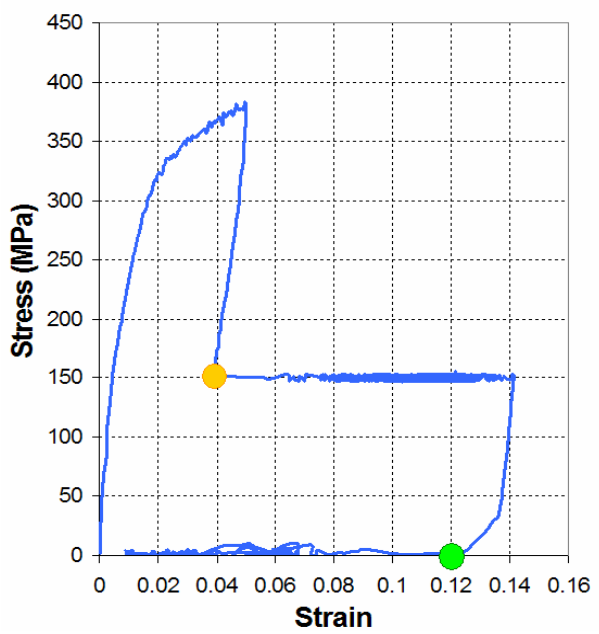

Figure 4a. Stress-strain diagram with 5% applied strain in martensite followed by isobaric cycling at 150 MPa. The test temperature was 260°C.

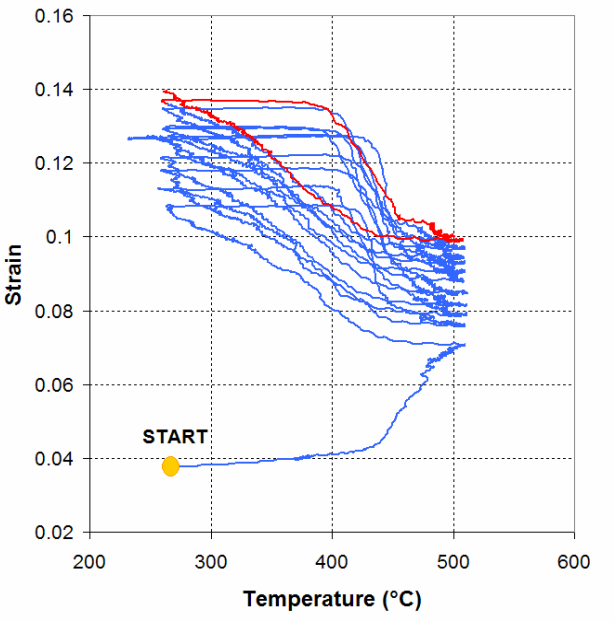

Figure 4b. Strain-temperature plot showing the isobaric transformation behavior under an applied stress of 150 MPa.

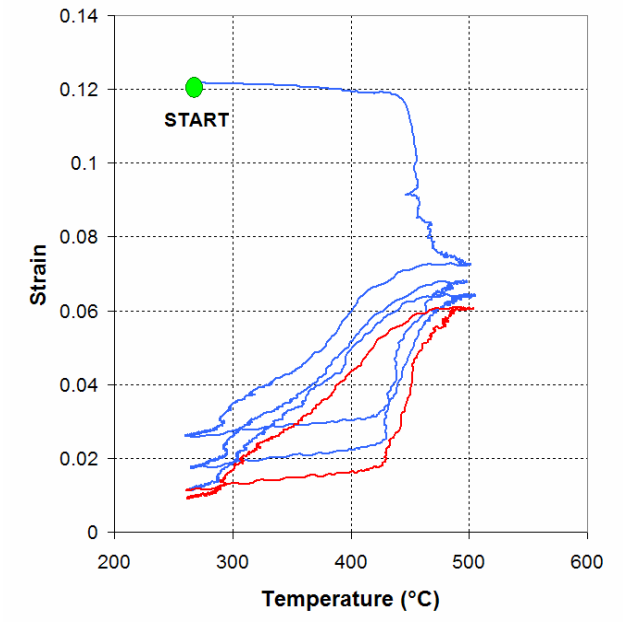

Figure 4c. Strain-temperature plot showing the isobaric transformation behavior under an applied stress of 0 MPa.

4. DISCUSSION

Recall that after isothermally loading the specimen at 260ºC, the material is unloaded to 150 MPa (see Figure 4a). The material is thermally cycled, with the stress held constant at 150 MPa. While heating above A_f in the first thermal cycle, the SMA expands by approximately 3%. The expansion of a SMA upon heating under tensile stress is uncommon behavior for a SMA. There is a further expansion of approximately 4% during cooling to 260ºC, which is conventional SMA tensile behavior. The nature of the behavior exhibited during this first thermal cycle under a stress of 150 MPa is unique compared to other SMAs. Such a unidirectional transformation behavior has been observed in CoNi single crystals [22]. The unidirectional strain generation was attributed to the multiple possibilities for the reverse transformation (martensite to austenite) to occur (through atomic rearrangement) resulting in the deformation to continue along the direction of applied stress. The transformation in CoNi was irrecoverable in nature and the deformation permanently ceased after a few cycles. In the current results observed in TiPdNi, the uncommon transformation occurs only during the first thermal cycle after which the material reverts to the conventional SMA behavior. Secondly, the large strains generated under stress are recovered during the first thermal cycle in the absence of stress. After this, the material exhibits *compressive* TWSME (expansion on heating and contraction upon cooling) with further thermal cycling under no load. In order to investigate this peculiar effect, an untested specimen was mounted on the frame and thermally cycled at zero stress. A partial compressive TWSME was observed in the material. The compressive TWSME observed in the specimen suggests presence of compressive favored variants inherently present in the specimen after processing. In order to study the crystal structure in detail, XRD study was performed on the material at two different stages. The first test was performed before testing the specimen. The second test was performed on unloading after performing one thermal cycle under stress of 150 MPa. In both cases the XRD pattern was indexed to a B19 (orthorhombic) structure with lattice parameters a=2.78Å, b=4.53Å and c=4.78Å. This is consistent with the other studies performed on this alloy composition [17, 23]. Figure 6 shows the XRD patterns before testing and after the first thermal cycle under stress. It is observed from the XRD patterns that the relative intensity of the peak [020] with respect to [111] has changed considerably from before and after the test, indicating an apparent change in the martensitic texture, which in turn is associated with the preferred variant generation.

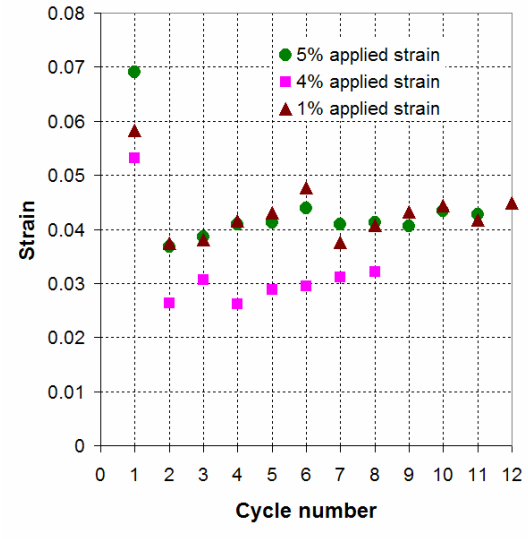

Figure 5. Transformation strain in each cycle under a stress of 150 MPa for different applied strain levels.

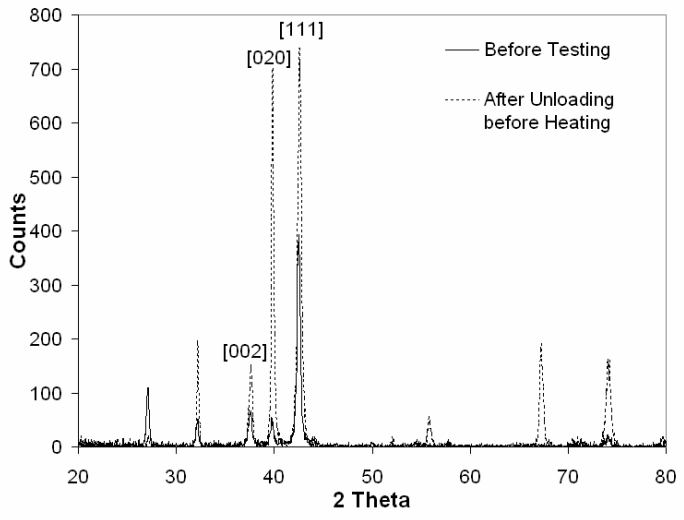

Figure 6. XRD data for the specimen before testing and after isothermal cycling under stress of 150 MPa.

Based on the observations from the test results and the XRD patterns the following behavior may be hypothesized. When the specimen is heated to a temperature above A_f, the compressive variants transform to austenite (causing expansion); however, the presence of the applied stress favors the formation of tensile favored martensitic variants from austenite

upon cooling causing a further expansion. After the initial thermal cycle the material exhibits conventional tensile SME behavior. After unloading, when the specimen is heated in the absence of stress, the tensile favored variants transform to austenite upon heating (thus contracting). Upon the final stress-free cooling, they revert to compressive martensitic variants from austenite (causing a further contraction) upon cooling. The nature of this "recoverable unidirectional transformation" and the added fact that several thermal cycles under constant stress in tension leaves this behavior unaffected suggests a very strong biasing mechanism at the microstructural level. Another key observation is the shape of the thermal hysteresis. It is noted (Figure 4b, 4c) that in all cases, the material exhibits a gradual forward transformation in contrast to a sharp reverse transformation causing a very unsymmetrical thermal hysteresis. Similar hysteretic curves have been observed in Ni rich-Ti binary SMA [24]. The lack of symmetry in the hysteresis occurs due to the difference in the energy required to initiate and propagate the transformation between the forward and reverse cases. From the strain temperature diagrams (4b, 4c) it is noticed that the forward transformation begins almost instantaneously but a high temperature is required to initiate the reverse transformation and the transformation occurs relatively fast. Detailed TEM studies will be necessary to determine the exact origin of this "recoverable unidirectional transformation" strain.

5. SUMMARY AND CONCLUSIONS

A detailed thermomechanical experimental study was performed on a nominal composition of $Ti_{50}Pd_{40}Ni_{10}$ specimens to study their actuation behavior in tension. The study revealed a unique unidirectional transformation behavior, which generates large transformation strains under stress and is recoverable under zero stress conditions. The compression TWSME observed in the tensile specimens at zero stress suggests a high fraction of compression favored martensitic variants instead of self accommodated martensitic variants. The large transformation strain behavior was attributed to the transformation of the inherent compressive favored variants to tension favored variants upon actuation and cooling under stress and vice versa in the stress free state. The strong biasing effect favoring the formation compressive variants is evident from the stability of the back transformation even after repeated thermal cycling in tension.

The behavior observed in $Ti_{50}Pd_{40}Ni_{10}$ HTSMA provides a means of generating large transformation strains under stress without permanently damaging the material. A total transformation strain of up to 7% is a significant improvement in the performance of high temperature actuation behavior. The material is also capable of resetting the shape in the stress free state. Further TEM studies and thermomechanical testing is necessary to determine the cause for this unique behavior. Studies will be performed to determine the effect of stress on the transformation strain behavior and to study the cyclic actuation behavior of the material.

ACKNOWLEDGMENTS

The authors would like to acknowledge the valuable discussions with Dr. Karaman of Mechanical Engineering at Texas A & M University.

REFERENCES

1. K. Otsuka, C. M. Wayman, "Shape Memory Materials", Cambridge University Press, Cambridge, 1999.
2. A. Srinivasan, D. McFarland, "Smart Structures: Analysis and Design", Cambridge University Press, Cambridge, 2001.
3. J. A. DeCastro, K. J. Melcher and R. D. Noebe, "System-Level Design of a Shape Memory Alloy Actuator for Active Clearance Control in the High-Pressure Turbine", NASA/TM—2005-213834, July 2005, AIAA–2005–3988.
4. A. Andersen, D. Pedersen, A. Sivertsen, and S. Sangesland, "Detailed study of shape memory alloys in oil well applications," SINTEF Petroleum Research, Trondheim, Norway, Tech. Rep. 32.0924.00/01/99, July 1999.

5. P.G. Lidquist and C.M. Wayman, "Shape memory and transformation behavior of martensitic Ti-Pd-Ni and Ti-Pt-Ni alloys, Engineering Aspects of Shape Memory Alloys", Ed. T. W. Duerig, K. N. Melton, D. Stöckel and C. M. Wayman, Butterworth-Heinemann, London, 129, 1990.
6. P. E. Thoma and J. J. Boehm, "Effect of composition on the amount of second phase and transformation temperatures of $Ni_xTi_{90-x}Hf_{10}$ shape memory alloys", Materials science and engineering A 273-275, 385-389, 1999.
7. S.K. Wu, and C.M. Wayman, "Martensitic Transformations and the Shape-Memory Effect in $Ti_{50}Ni_{10}Au_{40}$ and $Ti_{50}Au_{50}$ Alloys", Metallography, 20 (1987) 359.
8. Z. Pu, H. Tseng and K. Wu, "Martensite Transformation and Shape-Memory Effect of NiTi-Zr High- Temperature Shape-Memory Alloys", Smart Structures and Materials 1995: Smart Materials, SPIE Proc. Vol. 2441 (1995) 171.
9. T. Briggs, M. B. Cortie, M. J. Witcomb and L. A. Cornish, "Platinum Alloys for Shape Memory Applications", Platinum Metals Rev., 2003, 47, (4), 142-156.
10. H. C. Doonkersloot and Van Vucht, "Martensitic transformations in Au-Ti, Pd-Ti and Pt-Ti alloys", J. Less-Common Metals, 20, 83-91, 1970.
11. E. P. George, C. T. Liu, J. A. Horton, C. J. Sparks* M. Kao, H. Kunsmann and T. King. "Characterization, Processing, and Alloy Design of NiAI-Based Shape Memory Alloys", MATERIALS CHARACTERIZATION 32, 139-160, 1994.
12. K. Otsuka, K Oda, Y. Ueno and Min Piao, "The shape memory effect in a $Ti_{50}Pd_{50}$ alloy", Scripta Metallurgica et Materialia, Vol. 29, 1355-1358, 1993.
13. D. Goldberg, Y. Xu, Y. Murakami, K. Otsuka, T. Ueki and H. Horikawa, High-temperature shape memory effect in $Ti_{50}Pd_{50-x}Ni_x$ (x=10, 15, 20) alloys, Materials letters 22, 241-248, 1995.
14. T. Cheng, "High Temperature Shape Memory Effects of Ni-34.6at%Al with improved ductility and toughness", Scripta Metallurgica et Materialia, Vol. 31, No. 9, 1187-1192, 1994.
15. S. Shimizu, Y. Xu, E. Okunishi, S. Tanaka, K. Otsuka and K. Mitose, Improvement of shape memory characteristics by precipitation hardening of Ti-Pd-Ni alloys, Materials letters 34, 23-29, 1998.
16. P. K. Kumar, D. C. Lagoudas, K. J. Zanca, M. Z. Lagoudas, "Thermomechanical characterization of high temperature SMA actuators", Smart Structures and Materials 2006: Active Materials: Behavior and Mechanics, Proceedings of SPIE 6170, 306-312, 2006.
17. R. Noebe, S. Padula II, G. Bigelow, O. Rios, A. Garg and B. Lerch, "Properties of a $Ni_{19.5}Pd_{30}Ti_{50.5}$ high-temperature shape memory alloy in tension and compression", Smart Structures and Materials 2006: Active Materials: Behavior and Mechanics, Proceedings of SPIE, 6170, 279-291, 2006.
18. O. Rios, R. Noebe, T. Biles, A. Garg, A. Palczer, D. Scheiman, H.J. Seifert and M. Kaufman, "Characterization of ternary NiTiPt high-temperature shape memory alloys", Smart Structures and Materials 2006: Active Materials: Behavior and Mechanics, Proceedings of SPIE, 5761, pp. 376-387
19. S. Padula II, G. Bigelow, R. Noebe, D. Gaydosh, and A. Garg "Challenges and Progress in the Development of High-Temperature Shape Memory Alloys Based on NiTiX Compositions for High-Force Actuator Applications.", SMST 2006: Proceedings of the International Conference on Shape Memory and Superelastic Technologies. ASM International, Metals Park, OH (2006).
20. R. Noebe, S. Draper, D. Gaydosh, A. Garg, B. Lerch, G. Bigelow and S. Padula II, "Effect of Thermomechanical Processing on the Microstucture, Properties, and Work Behavior of a $Ti_{50.5}Ni_{49.5}Pt_{20}$ High-Temperature Shape Memory Alloy", SMST, 2006.
21. D. Hartl, B. Volk, D. C. Lagoudas, F. T. Calkins, and J. Mabe, "Thermomechanical Characterization and Modeling of Ni60Ti40 SMA for Actuated Chevrons", Proceedings of ASME, International Mechanical Engineering Congress and Exposition, 1-10, 2006.
22. Y. Liu, G. Tan, S. Miyazaki, Y. Liu and B. Jiang, "Thermomechanical behavior of FCC← →HCP martensitic transformation in CoNi", Journal of Physics IV, 112, 1025-1028, 2003.
23. J. Wu and Q. Tian, "The superelasticity of TiPdNi high temperature shape memory alloy", Intermetallics 11, 773-778, 2003.
24. H. Sehitoglu, R. Hamilton, H.J. Maier and Y. Chumlyakov, "Hysteresis in NiTi alloys", Journal of Physics IV, 115, 3-10, 2004.